RESEARCH PAPER

Geophysical assessment for the gas-bearing sandstones of the Pliocene Kafr El-Sheikh formation in Tao field, offshore Nile Delta Basin, Egypt

ElSayed Selim [a,b,*], Mohammad A. Sarhan [b], Adel A. Kushlaf [c], Ahmed Shalaby [d]

[a] Department of Physics, College of Science and Humanities, Al-Kharj, Prince Sattam Bin Abdulaziz University, Al-Kharj, Saudi Arabia
[b] Department of Geology, Faculty of Science, Damietta University, New Damietta, Egypt
[c] Department of Engineering Geology, Faculty of Oil and Gas, University of Zawia, Zawia, Libya
[d] Department of Geology, Faculty of Science, Mansoura University, El-Mansoura, Egypt

Abstract

The primary objective of this investigation is to conduct a petrophysical evaluation of the gas potential within the sandstones of the Pliocene Kafr El-Sheikh Formation (KSF) located in the Tao Field, offshore Nile Delta Basin (NDB). The analysis relies on nineteen seismic sections and wireline logs obtained from two deviated drilled wells, namely Tao-6 and Tao-8 wells. The seismic examination reveals the presence of several distinctive bright spots within the KSF. These bright spots represent favorable gas-bearing reservoirs in the study area. The examination of the well logging data indicates positive petrophysical indicators throughout the sandstones of the KSF in both Tao-6 and Tao-8 wells, suggesting their potential as gas reservoirs. In the Tao-8 well, two notable pay intervals (Zone A and Zone B) were observed, displaying significant net pay vertical thickness varying between 57 m (in Zone A) and 60 m (in Zone B), effective porosity ranging from 34 to 37%, minimal shale content between 10 and 15%, low water saturation varying from 2 to 10%, high hydrocarbon saturation ranging from 90 to 98% and a low bulk volume of water varying between 1 and 4%. Meanwhile, the interpreted reservoir zone in the Tao-6 well (Zone C) is 6 m thick and exhibits an average effective porosity of 25%, low shale content of 20%, low water saturation of 3%, hydrocarbon saturation of 97%, and low bulk volume of water of 1%. The identified reservoir intervals within the Tao-6 and Tao-8 wells signify gas potential in the sandstones of the KSF in the offshore Nile Delta Basin, providing valuable insights for future gas exploration, especially in the neighboring regions of the study area.

Keywords: Bright spot, Gas-bearing sandstones, Pliocene sequence, Shallow reservoirs, Tao field

1. Introduction

The Neogene to Quaternary segment of the Nile Delta Basin (NDB) has garnered significant attention in hydrocarbon exploration due to its abundant gas reserves.[1,2] Exploration efforts have targeted both onshore and offshore areas. Over the past five decades, the NDB has emerged as a major gas-producing region, with the discovery of numerous trillion cubic feet of gas. These discoveries span various geological layers, from the Oligocene to the Pliocene-Pleistocene.[3–10] The exploration history in the NDB underscores its importance as a prolific source of gas reservoirs across diverse geological formations. The Abu Madi Formation, in particular, has served as a significant natural gas source for numerous petroleum companies operating in both onshore and offshore regions of the NDB since 1963, as documented by Abu El-Ella.[11] Generally, well logging is a critical tool in the exploration and appraising the hydrocarbon potential in oil and gas reservoirs.[12–23] In this study, the geophysical assessment of gas-bearing sandstones was conducted through a petrophysical evaluation of the

Received 24 April 2024; revised 1 June 2024; accepted 7 July 2024.
Available online 27 August 2024

* Corresponding author at: Department of Physics, College of Science and Humanities, Al-Kharj, Prince Sattam Bin Abdulaziz University, Al-Kharj 11942, Saudi Arabia.
E-mail address: e.selim@psau.edu.sa (E. Selim).

https://doi.org/10.62593/2090-2468.1040

Pliocene Kafr El-Sheikh reservoirs in the Tao field, primarily using wireline logs.

The NDB is identified as a passive margin basin, originating from thermal subsidence following extension tectonics that detached the African and the Eurasian plates during the Late Triassic-Early Cretaceous period.[24,25] It exhibits a fan-shaped structure and encompasses a significant sedimentary section spanning from the Late Tertiary up to the Quaternary age, covering approximately 250 000 km^2 in the eastern Mediterranean region. The basin's geological history includes the formation of a significant faulted and overall flexed zone known as the Hinge Zone during the Jurassic to Early Cretaceous period. This geological feature extends across northern Egypt and has been documented by researchers such as Sestini and Said.[26,27] The Hinge Zone represents a notable tectonic element that influenced the geological characteristics of the NDB during this specific time frame. It serves as a distinctive marker for the southern boundary of the rifted continental margin in northern Egypt[28] and bisects northern Egypt along an east-west trending direction.[29] Along this hinge line, numerous normal faults have emerged, displaying a pronounced downward faulting trend toward the north. This geological activity has led to a notably thick sedimentary section, ranging between 5000 and 7000 m observed to the north of the line. In contrast, the southern side of this line records a considerably thinner section, ranging from 500 to 1500 m.[30,31,61] These observations underscore the significant impact of tectonic forces and faulting processes along the hinge line, influencing the thickness and structural characteristics of the sedimentary deposits on either side of this geological feature. During the Plio-Pleistocene epoch, a compression belt emerged, characterized by sinistral wrench tectonic, resulting in the development of the Pelusium fault, trending in a northeast-southwest direction. The Pelusium fault line traverses the northwestern offshore regions of Sinai, serves as a boundary for the southern portion of the NDB, and further extends into the western portion of the African Plate. This tectonic feature illustrates the dynamic geological processes that have influenced the structural development of the region during the specified period, reflecting the intricate interplay of forces along the Pelusium fault line.[32,61]

The Neogene section in the NDB (Fig. 1) includes the El Wastani and Mit Ghamr formations (Late Pliocene), Early-Middle Pliocene Kafr El-Sheikh Formation (KSF), Rosetta Formation (Messinian), Abu Madi Formation (Messinian), Qawasim Formation (Messinian), and Sidi Salim Formation (Serravallian-Tortonian).[33,34,61] The Rosetta Formation exhibits a relatively widespread distribution across the NDB; however, it is notably absent in the Abu Madi depositional systems, which encompasses fluvial to shallow marine environments.[60] This absence suggests distinct depositional settings and sedimentary conditions between the Rosetta Formation and the Abu Madi Formation, highlighting the complexity and variability of sedimentary processes in the NDB during the specified geological timeframe. The Abu Madi Formation primarily comprises sandstones and shales intercalations and was deposited during the Late Miocene (Messinian) age, specifically during the ending stage of the Upper Miocene syn-rift megasequence, as highlighted by EI-Heiny and Morsi; Egyptian General Petroleum (EGPC).[35,61] The deposition of the Abu Madi Formation was notably influenced by tectonic processes rather than changes in relative sea levels.[36]

The offshore region of Sinai (eastern NDB) holds favorable conditions for gas accumulation, necessitating intensified exploration efforts, as noted by Abd-Allah et al.[37] Additionally, the Pliocene-Pleistocene section in the TAO Field shows promise for hosting shallow gas reservoirs near existing hydrocarbon discoveries, warranting further investigation.[38] Therefore, this study purposes to evaluate the hydrocarbon potential of the sandy intervals of the Pliocene KSF in the Tao Field (Fig. 2). To achieve this objective, petrophysical parameters for the Pliocene sandstones in two wells in the Tao Field (Tao-6 and Tao-8) were evaluated. This assessment aids in determining the superiority of the gas reservoirs as well as contributes extra commercial gas reserves within the eastern offshore NDB.

2. Data and methodology

The current study is dedicated to the geophysical evaluation of the gas-bearing sandstones of the Pliocene KSF in Tao Field, offshore NDB (Fig. 2a). The available geophysical data comprises nineteen seismic profiles that span the studied area (Fig. 2b). Moreover, the mud logs as well as the conventional wireline logs from two deviated wells – Tao-6 and Tao-8 form the primary dataset for analysis (Figs. 3–5). This research focuses on calculating key petrophysical parameters essential for characterizing the gas-bearing zones within the studied wells. These parameters include water saturation (Sw), hydrocarbon saturation (Sh), bulk volume of water (BVW),

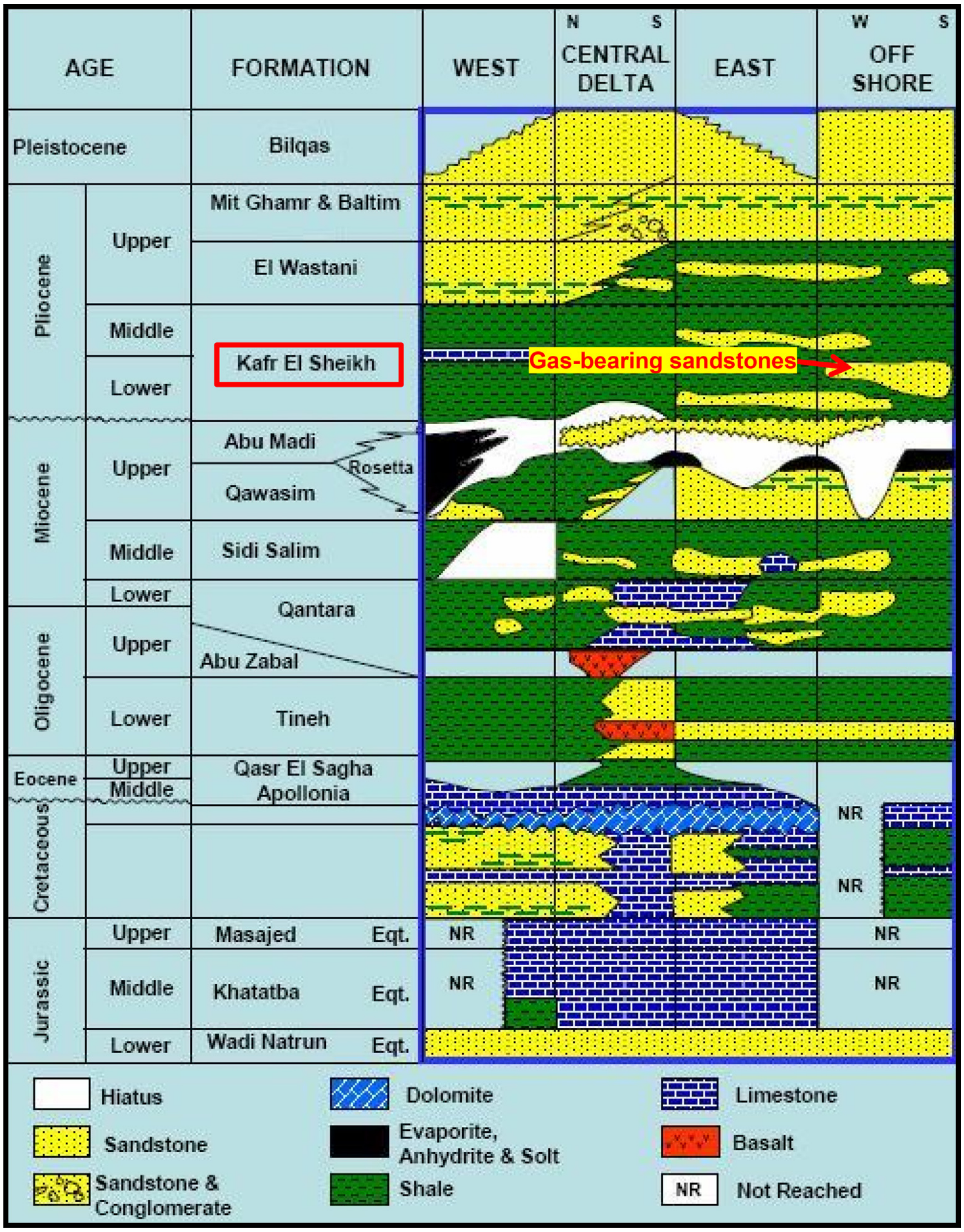

Fig. 1. General lithostratigraphic column of the Nile Delta Basin, after.[4]

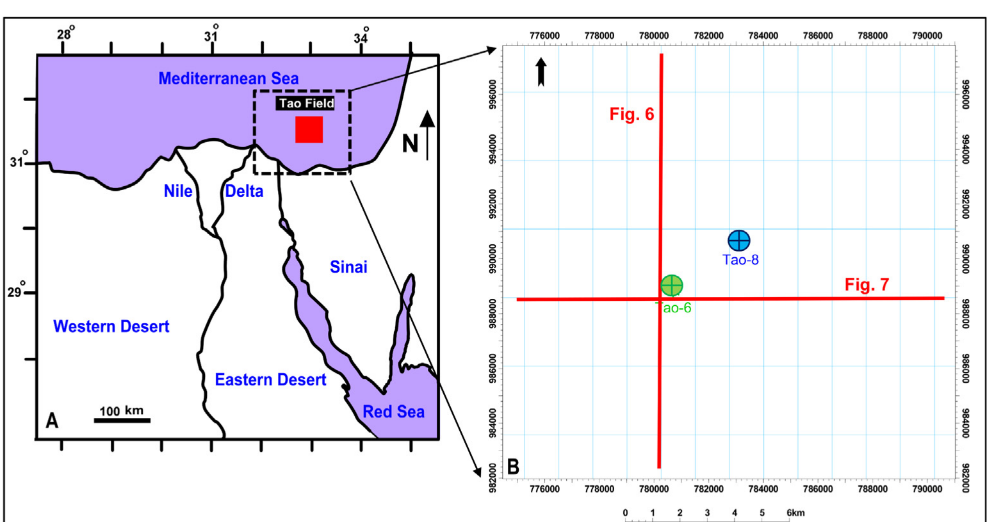

Fig. 2. (a) Map indicates the site of Tao Field, offshore Sinai. (b) Study area including wells locations and accessible seismic data.

effective porosity (PHIE), total porosity (PHIT) and shale content (Vsh) which was estimated using gamma ray (GR) wireline in each well. The shale content, total porosity and effective porosity were calculated using the equations of Asquith and Gibson[39] as follow:-

$$VSh = (GR - GR\min)/(GR\max - GR\min) \quad (1)$$

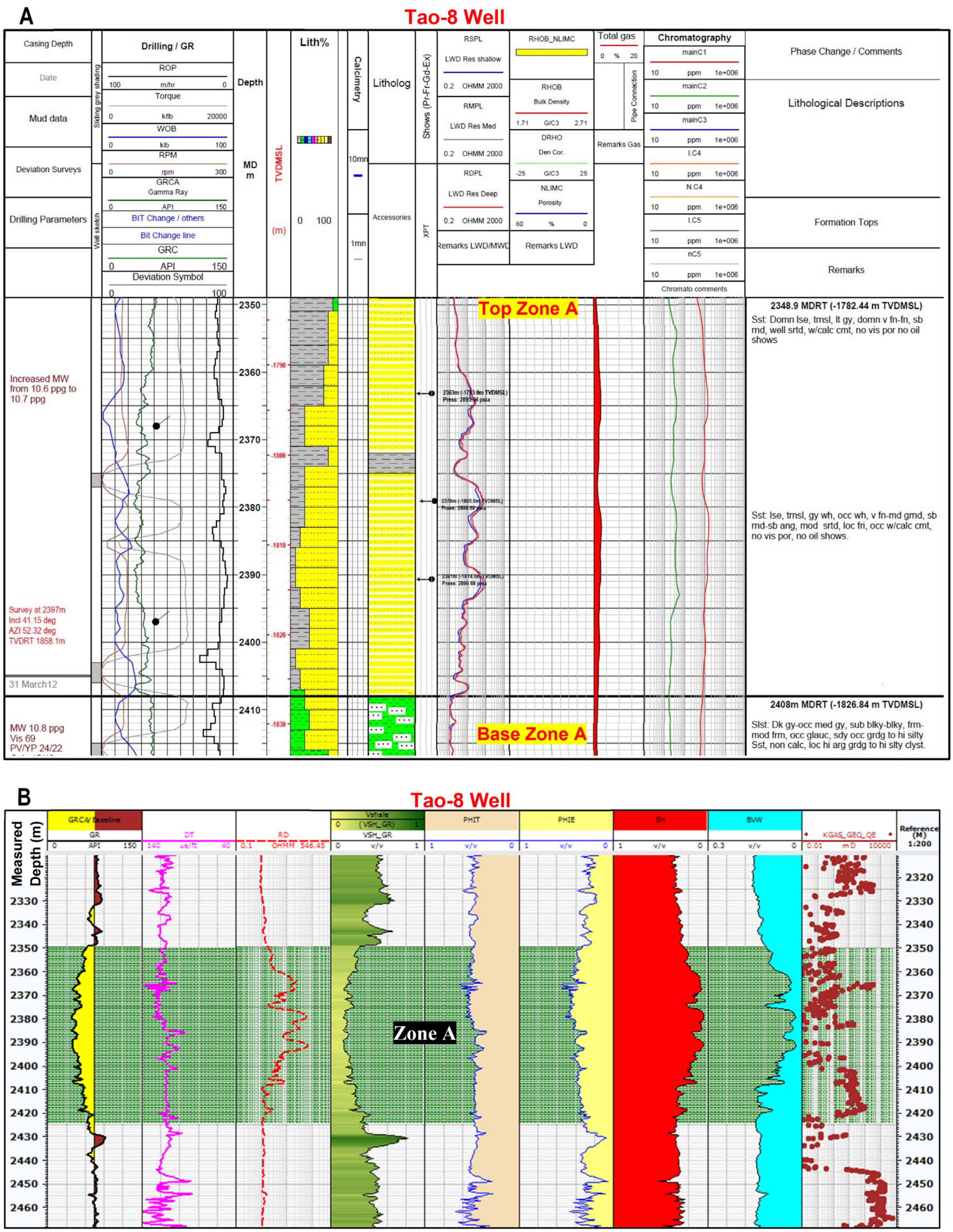

Fig. 3. (a) The mud log of Zone A in Tao-8 well shows the high values of the gas chromatographic analysis opposite Zone A. (b) Petrophysical data with evaluation for Zone A.

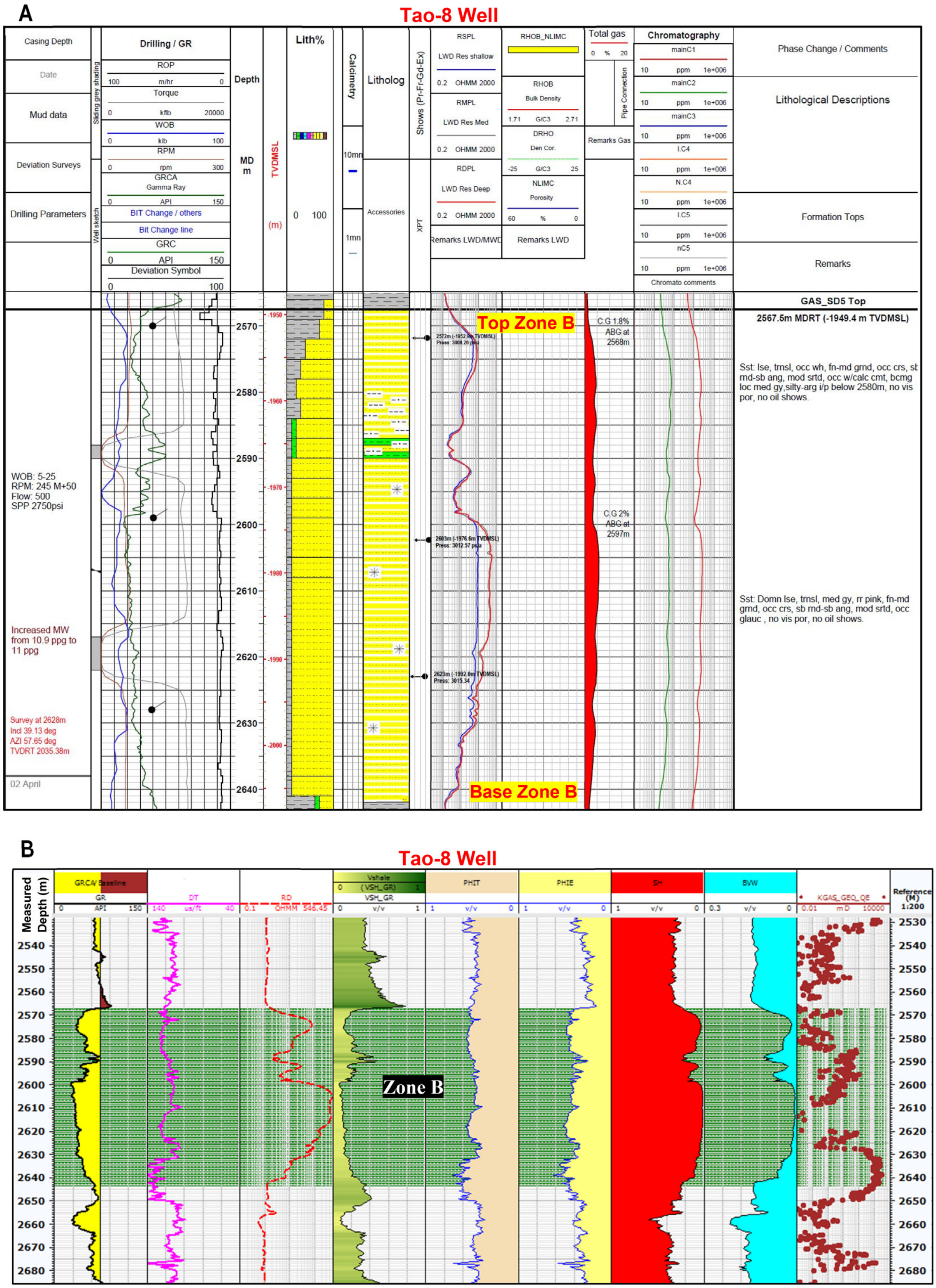

Fig. 4. (a) The mud log of Zone B in Tao-8 well shows the high values of the gas chromatographic analysis opposite Zone B. (b) Petrophysical data with evaluation for Zone B.

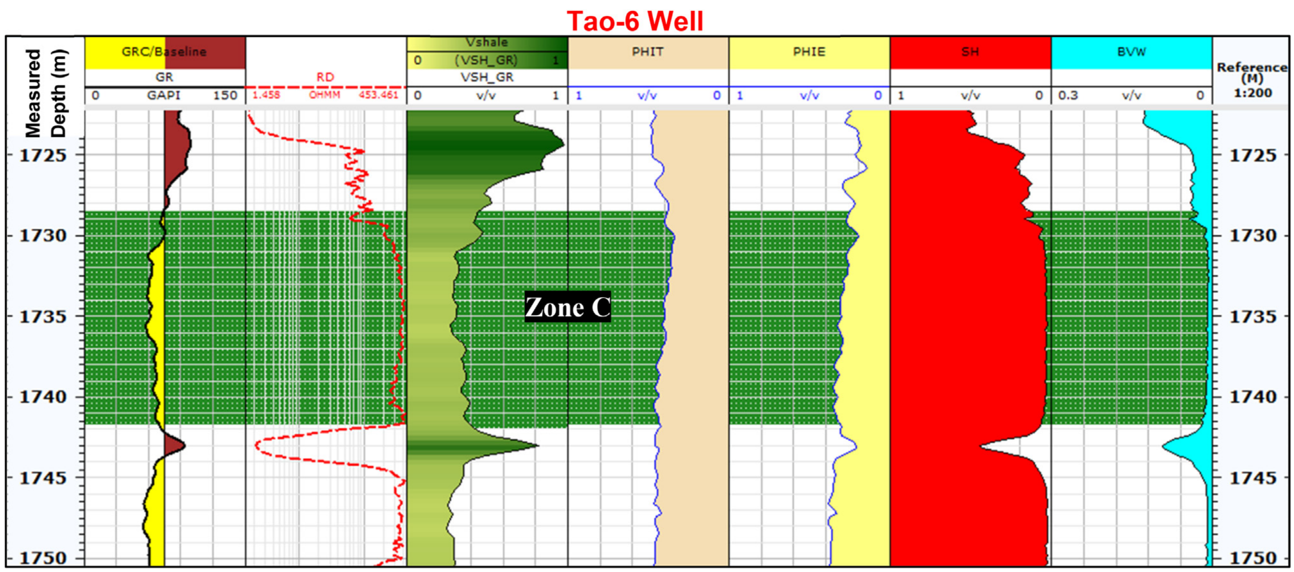

Fig. 5. Petrophysical data with evaluation for Zone C in Tao-6 well.

Where; V_{Sh} is shale content; GR is gamma ray reading; GR_{min} is the minimum gamma ray reading; and GR_{max} is the maximum reading.

$$\Phi T = (\Phi N + \Phi D)/2 \quad (2)$$

Where; Φ_T is total porosity; Φ_N is neutron porosity; Φ_D is the density porosity.

$$\Phi D = (\rho ma - \rho b)/(\rho ma - \rho fl) \quad (3)$$

Where; Φ_D is porosity derived from density log; ρ_b is bulk density; ρ_{ma} is density of matrix; ρ_{fl} is density of fluid.

$$\phi e = \phi T * (1 - VSh) \quad (4)$$

Where; ϕ_e is effective porosity, ϕ_T is total porosity; V_{Sh} is shale content.

On the other hand, the water saturation has been inferred following the Indonesian model[40] as follow:-

$$S_w = \left\{ \left[\left(\frac{V_{Sh}^{2-V_{Sh}}}{R_{Sh}} \right)^{\frac{1}{2}} + \left(\frac{\phi_e^m}{R_w} \right)^{\frac{1}{2}} \right]^2 R_t \right\}^{\frac{-1}{n}} \quad (5)$$

Where, S_w is water saturation; ϕ_e is effective porosity; V_{Sh} is shale content; R_{Sh} is shale resistivity taken as 5 Ωm; R_t is deep resistivity, R_w is water resistivity taken as 0.03 Ωm; 'm' and 'n' are cementation exponent and saturation exponents, respectively, with assumed value of 2.

While, the bulk volume of water was determined by applying the equation of Buckles.[41]

$$BVW = \phi e \times Sw \quad (6)$$

Where; ϕe = Effective porosity; Sw = water saturation.

This applied workflow was published by many authors.[42–48] The cut-off values which were applied in this work for delineating the pay zones in the examined wells are; water saturation <30%, hydrocarbon saturation >70%, effective porosity >15%, bulk volume of water >6% and shale volume <25%.

3. Results and discussion

The examination of the well logs data for the available two wells has confirmed that the sandstones of the Pliocene KSF in Tao Field exhibit favorable conditions to be considered as possible gas reservoirs in the two examined wells. The first interpreted pay interval of Tao-8 well (Zone A) is located between measured depths; 2350–2423 m (i.e. between true vertical depths; 1783–1840 m) (Fig. 3a) and the second interval (Zone B) is located between measured depths; 2568–2642 m (i.e. between true vertical depths; 1950–2010 m) (Fig. 4a). However, the deduced pay zone of Tao-6 well (Zone C) locates between measured depths; 1729–1742 m (i.e. between true vertical depths; 1058–1064 m) (Fig. 5). This conclusion is supported by several encouraging indicators, such as; the existence of higher values of the gas chromatographic analysis opposite these intervals in the available mud logs. Moreover, the examination of the well logs data revealed the clean nature (low mud content) of these intervals, evidenced by the low GR readings. Also, the high values of the deep resistivity curve reflecting the presence of gas.

The calculated key petrophysical parameters for Zone A and Zone B in the Tao-8 well (Figs. 3B & 4B) show an average total porosity of 40%. The effective porosity ranges between 34% and 37%, the shale volume fluctuates between 10% and 15%, and the water saturation values vary between 2% and 10% (i.e., the gas saturation varies between 90% and 98%) with a low bulk volume of water fluctuating between 1% and 4%. On the other hand, the calculated petrophysical properties for Zone C in the Tao-6 well display a total porosity varying between 33% and 37%, while the effective porosity ranges between 22% and 28%. The shale volume fluctuates between 15% and 25%, the water saturation values vary between 2% and 4% (i.e., the hydrocarbon saturation varies between 96% and 98%), and there is a low bulk volume of water, averaging 1%.

On the other hand, the sands within the gas-bearing zones of the KSF, as indicated by mud logs, exhibit similar characteristics. They are loose and variable in texture from medium to fine-grained, occasionally appearing coarse. Color-wise, they

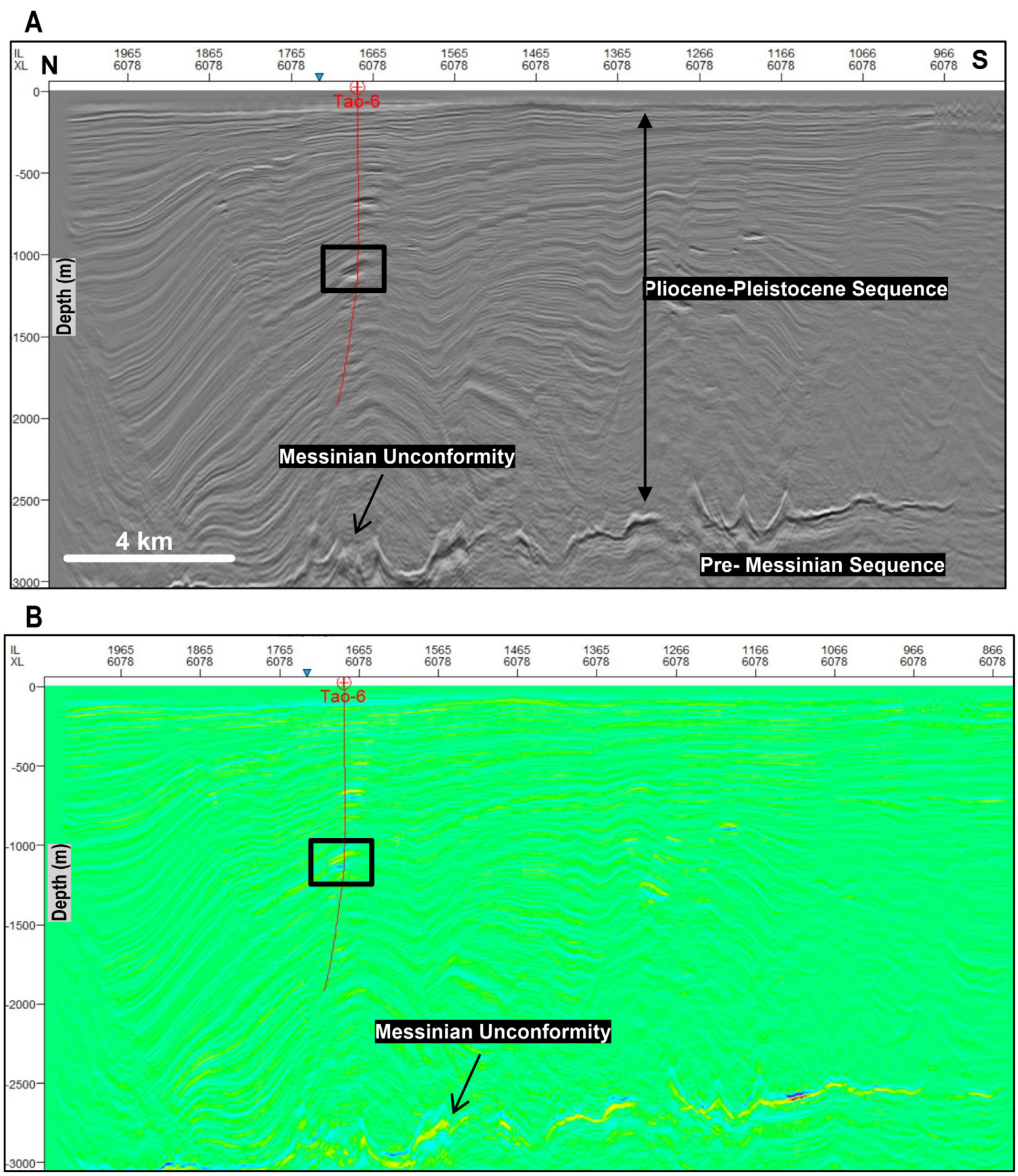

Fig. 6. N–S seismic line no. XL 6078 shows the Pliocene-Pleistocene sequence and the gas-bearing interval in Tao-6 well (i.e. Zone C) outlined by the black square. (a) The seismic line in black-grey-white color. (b) The seismic line after applying the frequency attribute to observe the appearance of the reservoir zone (Zone C) as a distinctive bright spot.

range from colorless to white or grey. Their grains typically have a sub-rounded to sub-angular shape. The sorting is moderate to well, suggesting some level of uniformity in grain size. Additionally, these sands are glauconitic in nature.

On seismic sections, these gas-bearing zones appear as bright spots (Figs. 6 and 7). These bright spots represent the supreme common characteristics of the Direct Hydrocarbon Indicators (DHI). The Direct Hydrocarbon Indicators indicates the presence of oil and gas on seismic data and reduces the penetrating risk for dry exploration wells.[49] The observed bright spots on the examined seismic data (Figs. 6 and 7) were resulted from the fluctuations in seismic wave amplitude, a phenomenon influenced by the physical characteristics of the rock and the fluids it contains, as outlined by Gardner et al.[50]

In the NDB, the shallow Pliocene gas-bearing sandstones are identifiable by distinct direct indicators of hydrocarbons, such as flat and bright spots observed on seismic data. These indicators have significantly increased the success rate in the industry, reaching around 90%, as reported by Samuel et al. and Dolson et al.[51,52] In the offshore Sinai, numerous bright spots have been drilled within the Pliocene layers overlying the Messinian

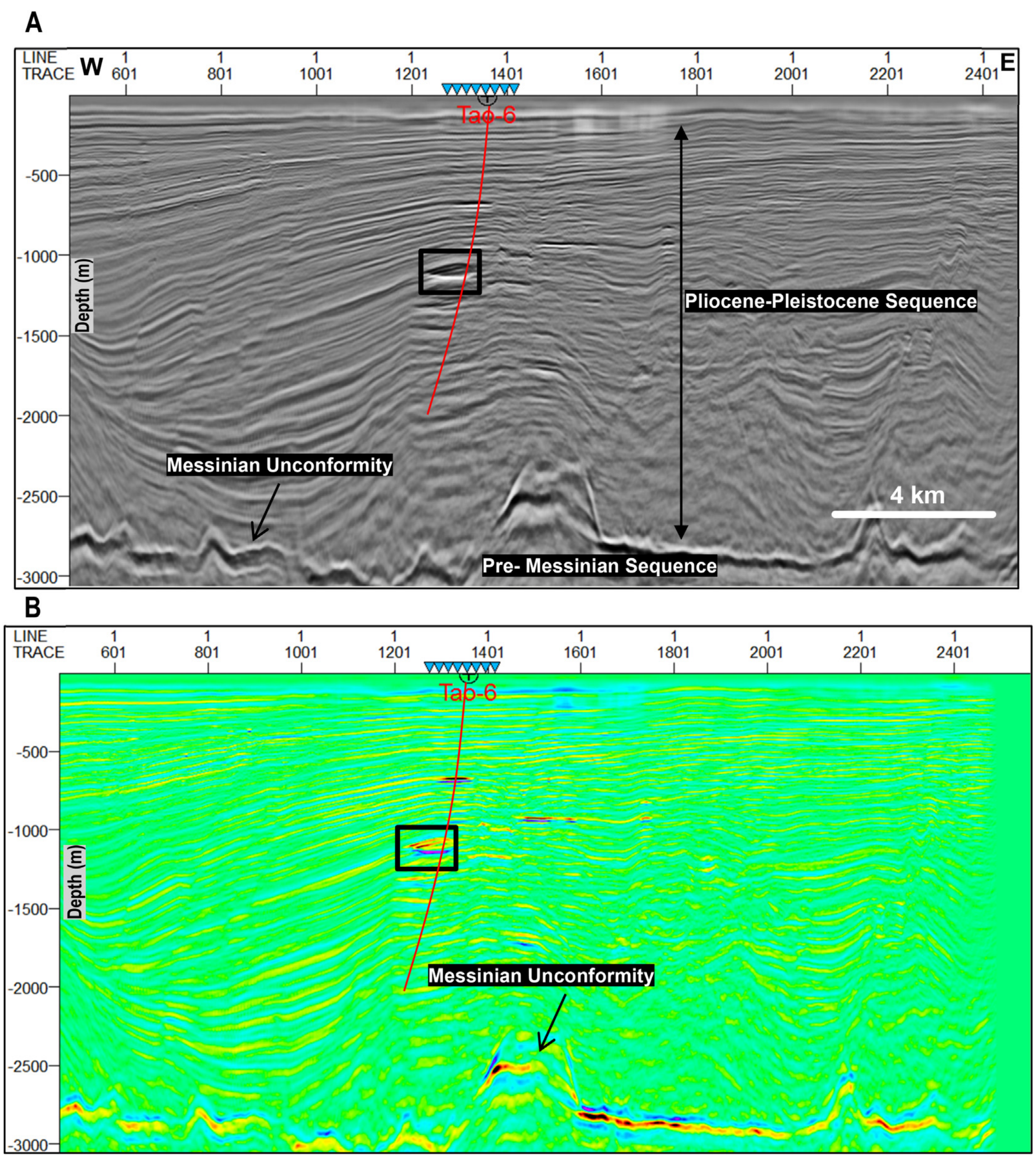

Fig. 7. E–W seismic line no. IL 1685 shows the reservoir interval of Zone C in Tao-6 Well (Black square). (a) The seismic line in black-grey-white color. (b) The seismic line after applying the frequency attributes.

evaporites, resulting in confirmed gas discoveries, as documented by Ewida and Darwesh.[38] In the offshore NDB, the Pliocene hydrocarbon reservoirs are anticipated to contain primarily biogenic gas, which is sourced from the Pliocene shale found in the KSF.[34,53]

Generally, the sandstones of the KSF, along with the sandstones of the El-Wastani Formation, are identified as the greatest promising goals for gas production in the offshore regions of the NDB and forming thick reservoirs.[54] This assertion is supported by studies conducted by Lashin and Mogren; Othman et al.; Abd El-Gawad et al.; Leila and Mohamed; Elatrash et al.[55–59] Consequently, the attractiveness of these formations lies in the fact that the Pliocene sequence in the Tao field, offshore the NDB presents fewer challenges in terms of exploring new gas reservoirs.

4. Conclusions

(a) The sandstones of the Lower-Middle Pliocene KSF represent promising potential shallow gas reservoirs in the offshore NDB.
(b) The geophysical assessment exhibits optimistic petrophysical signs for the sandstones of the KSF in the Tao field being possible reservoirs. The examined reservoirs exhibit significant characteristics, including net pay thickness ranging from 6 m to 60 m, effective porosity varying between 25 and 37%, shale content fluctuating from 10 to 20%, water saturation ranging from 3 to 10%, gas saturation varying between 90 and 97% and bulk volume of water varying between 1 and 4%.
(c) The multiple and thick gas intervals within the Tao-8 well highly recommend drilling deviated wells to allow companies to intersect more productive zones within the reservoir, increasing production from a single wellbore.
(d) The interpreted reservoir zones are commonly represented by 'bright spots' on seismic sections, therefore, the high-quality seismic data is critical in the exploration and production of gas reserves in Tao field and surrounds.
(e) It is highly recommended to drill new shallower wells in the Tao field and surroundings to discover extra potential gas-bearing reservoirs within the KSF.

Ethical statement

We certify that this manuscript has not been published before or being considered for publication anywhere.

Funding

This study is supported via funding from Prince Sattam bin Abdulaziz University project number (PSAU/2024/R/1445).

Acknowledgments

This study is supported via funding from Prince Sattam Bin Abdulaziz University project number (PSAU/2024/R/1445). The authors are also grateful to the Egyptian General Petroleum Corporation (EGPC) and the North Sinai Petroleum Company (NOSPCO) for providing the geophysical data. The authors are also thankful to Ms. Asmaa Elsayed Ahmed Elmenier, the researcher in Geology Department, Faculty of Science at Damietta University for helping in obtaining the geophysical data. Many thanks for Eng. Soliman and Eng. M. EL-Maghraby at NOSPCO for the continuous help and fruitful discussions during the processing of the present work.

Author's contribution

All authors have equal contributions.

Data availability

The used geophysical data is confidential.

Conflicts of interest

There are no conflicts of interest.

References

1. El-Fawal FM, Sarhan MA, Collier REL, Basal A, Aal MHA. Sequence stratigraphic evolution of the post-rift megasequence in the northern part of the Nile Delta Basin, Egypt. *Arabian J Geosci*. 2016;9:585.
2. Sarhan MA, Safa MG. 2D seismic interpretation and hydrocarbon prospects for the Neogene-Quaternary succession in the Temsah Field, offshore Nile Delta Basin, Egypt. *J Afr Earth Sci*. 2019;155:1–12.
3. Nabawy BS, Shehata AM. Integrated petrophysical and geological characterization for the Sidi Salem-Wakar sandstones, offshore Nile Delta, Egypt. *J Afr Earth Sci*. 2015;110:160–175.
4. Sarhan MA. Assessing hydrocarbon prospects in Abu Madi formation using well logging data in El-Qara field, Nile Delta Basin, Egypt. *J Pet Explor Prod Technol*. 2021;11:2539–2559.
5. Assal EM, Farouk S, Sarhan MA. Sedimentary facies controls on reservoir quality of the Abu Madi Formation, offshore Nile Delta Basin, Egypt. *Geomech Geophys Geo-Energy Geo-Resour*. 2023;9:130.
6. Nabawy BS, Abd El Aziz EA, Ramadan M, Shehata AA. Implication of the micro- and lithofacies types on the quality of a gas-bearing deltaic reservoir in the Nile Delta, Egypt. *Sci Rep*. 2023;13:8873.
7. Abdel-Fattah MI, Hamdan HA, Sarhan MA. Hydrocarbon potential and reservoir characteristics of incised-valley transgressive sandstones: a case study of the Messinian gas reservoirs (Nile Delta Basin, Egypt). *J Afr Earth Sci*. 2023;207:105073.
8. Shehata AA, Sarhan MA, Abdel-Fattah MI, Assal EM. Sequence stratigraphic controls on the gas-reservoirs distribution and

characterization along the Messinian Abu Madi incision, Nile Delta Basin. *Mar Petrol Geol*. 2023;147:105988.
9. Eysa EA, Nabawy BS, Ghoneimi A, Saleh AH. Petrophysical rock typing based on the diagenetic effect of the different microfacies types of Abu Madi clastic reservoir in Faraskur Gas Field, onshore Nile Delta, Egypt. *J Pet Explor Prod Technol*. 2024;14:381–406.
10. Farouk S, Sen S, Sarhan MA, et al. Petrographical, petrophysical, and geomechanical characterization of the Pliocene sandstone reservoirs of the Scarab Gas Field, deepwater Nile Delta, Egypt – inferences on reservoir development. *J Afr Earth Sci*. 2024;214:105259.
11. Abu El-Ella R. The Neogene-Quatemary section in the Nile Delta, Egypt; Geology and hydrocarbon potential. *J Petrol Geol*. 1990;13:329–340.
12. Baouche R, Nabawy BS. Permeability prediction in argillaceous sandstone reservoirs using fuzzy logic analysis: a case study of Triassic sequences, Southern Hassi R'Mel Gas Field, Algeria. *J Afr Earth Sci*. 2021;173:104049.
13. Cherana A, Aliouane L, Doghmane MZ, Ouadfeul S-A, Nabawy BS. Lithofacies discrimination of the Ordovician unconventional gas-bearing tight sandstone reservoirs using a subtractive fuzzy clustering algorithm applied on the well log data: Illizi Basin, the Algerian Sahara. *J Afr Earth Sci*. 2022;196:104732.
14. Nabawy BS, Lashin AA, Barakat MK. Implementation of lithofacies and microfacies types on reservoir quality and heterogeneity of the late cretaceous upper bahariya member in the shurouk field, shoushan basin, North Western Desert, Egypt. *J Asian Earth Sci*. 2022;224:105014.
15. Farouk S, Sen S, Pigott JD, Sarhan MA. Reservoir characterization of the middle Miocene Kareem sandstones, Southern Gulf of Suez Basin, Egypt. *Geomech Geophys Geo-Energy Geo-Resour*. 2022;8:130.
16. Farouk S, Sen S, Belal N, Omran MA, Assal EM, Sarhan MA. Assessment of the petrophysical properties and hydrocarbon potential of the lower Miocene Nukhul formation in the Abu Rudeis-Sidri Field, Gulf of Suez Basin, Egypt. *Geomech Geophys Geo-Energy Geo-Resour*. 2023;9:36.
17. Mohamed AS, Omran AA, Mohamed MT, Nabawy BS. Petrophysical analysis and hydrocarbon potential of the Matulla Formation in the Muzhil Field, central part of the Gulf of Suez, Egypt. *Min Miner Depos*. 2023;17:2.
18. Shehata AA, Abdel-Fattah MI, Hamdan HA, Sarhan MA. Seismic interpretation and sequence stratigraphic analysis of the Bahariya Formation in the South Umbaraka oilfields (Western Desert, Egypt): insights into reservoir distribution, architecture, and evaluation. *Geomechanics Geophys Geo-Energy Geo-Resources*. 2023;9:135.
19. Belal N, Farouk S, Wady M, Sarhan MA, Assal EM. Biostratigraphy of the lower Miocene Nukhul Formation, Gulf of Suez, Egypt. *Sci J Damietta Fac Sci*. 2024;14:91–99.
20. Sarhan MA, Abdel-Fattah MI. Integrating well logs and seismic data for a comprehensive geophysical appraisal of post-Albian oil reservoirs in the SWQ-4X well, Gindi Basin, Egypt. *Egypt J Pet*. 2024;33:2.
21. Selim ES, Sarhan MA. Petrophysical evaluation of the pre-rift hydrocarbon reservoirs in the Gulf of Suez Basin. *Egypt J Pet*. 2024;33:100–108.
22. Farouk S, Qteishat A, Sen S, et al. Characterization of the gas-bearing tight paleozoic sandstone reservoirs of the risha field, Jordan: inferences on reservoir quality and productivity. *Arabian J Sci Eng*. 2024:1–21, under press.
23. Farouk S, Sen S, Saada SA, et al. Preliminary assessment of the Cambro-Ordovician reservoir potential from the Shushan basin, north Western Desert, Egypt. *J Afr Earth Sci*. 2024;213:105233.
24. May PR. The eastern mediterranean mesozoic basin: evolutionand oil habitat. *AAPG (Am Assoc Pet Geol) Bull*. 1991;75:1215–1232.
25. Dolson JC, Shann MV, Matbouly S, Harwood C, Rashed R, Hammouda H. *AAPG Memoir 74, Chapter 23: The Petroleum Potential of Egypt*. 2001.
26. Sestini G. *Nile Delta: A Review of Depositional Environments and Geological History*vol. 41. Geological Society, London, Special Publications; 1989:99–127.
27. Said R. *Geology of Egypt*. Balkema; 1990:734.
28. Bertello F, Barsoum K, Dalla S, Guessarian S. Temsah discovery: a giant gas field in a deep sea turbidite environment. In: *13th EGPe petroleum Conf. Explor Cairo, Egypt*. 1. 1996:165–180.
29. Mosconi A, Rebora A, Venturino G, Bocc P, Khalil M. Egypt-Nile Delta & North Sinai Cenozoic tectonic evolutionary model: a proposal. In: *13th EGPC petroleum Conf. Explor. Cairo, Egypt*. 1. 1996:203–223.
30. Harms JC, Wray JL. Nile delta. In: Said R, ed. *Geology of Egypt*. Rotterdam, Netherlands: AlBalkema; 1990:329–343.
31. Sarhan M, Hemdan K. North Nile Delta structural setting and trapping mechanism, Egypt. In: *12th EGPC petroleum Conf. Explor, Cairo, Egypt*. 1. 1994:1–18.
32. Zaghloul ZM, Shaaban F, Yossef A. Mesozoic and Cenozoic sedimentary basins of the Nile Delta, Egypt. In: Zaghloul ZM, Elgamal M, eds. *Deltas Modem and Ancient*. Cairo, Egypt: Proc. Mansoura Univ. 1st Internat. Symp. on Deltas; 2001:21–33.
33. EI-Heiny I, Enani N. Regional stratigraphic interpretation of Neogene sediments, Northern Nile Delta. In: *13th EGPC petroleum Conf., Explor., Cairo. Egypt*. 1. 1996:270–290.
34. Vandré C, Cramer B, Gerling P, Winsemann J. Natural gas formation in the western Nile delta (Eastern Mediterranean): thermogenic versus microbial. *Org Geochem*. 2007;38:523–539.
35. EI-Heiny I, Morsi S. Stratigraphic correlation of Neogene sediments in the eastern Nile Delta and Gulf of Suez. In: *11th Exploration and Production Conf Cairo*. 1. 1992:166–193.
36. Sarhan MA, Collier REL, Basal A, Aal MHA. Late Miocene normal faulting beneath the northern Nile Delta: NNW propagation of the Gulf of Suez Rift. *Arabian J Geosci*. 2014;7:4563–4571.
37. Abd-Allah AM, Abd El-Naby A, Aal MHA. Tectonic and basin evolution of South Eastern Mediterranean for hydrocarbon potentiality in North Sinai, Egypt. *J Pet Sci Eng*. 2020;190:107080.
38. Ewida HF, Darwesh MS. *Hydrocarbon Plays and Prospectivity from Possible Seismic Hydrocarbon Indicators in Offshore North Sinai*. Alexandria, Egypt: MOC; 2010.
39. Asquith G, Gibson C. Basic well log analysis for geologists: methods. In: *Exploration Series*. Tulsa, Oklahoma: AAPG; 1982.
40. Poupon A, Leveaux J. Evaluation of water saturation in shaly formations. In: *SPWLA 12th Annual Logging Symposium*. Society of Petrophysicists and Well-Log Analysts; 1971.
41. Buckles RS. Correlating and averaging connate water saturation data. *J Can Petrol Technol*. 1965;4:42–52.
42. Nabawy BS. Impacts of dolomitization on the petrophysical properties of El-Halal Formation, North Sinai, Egypt. *Arabian J Geosci*. 2013;6:359–373.
43. Sarhan MA, Basal AMK, Ibrahim IM. Seismic and well logging interpretation for evaluation of the lower Bahariya reservoir, southwest Qarun (SWQ) Field, Gindi Basin, Egypt. *Mar Geophys Res*. 2017;38:271–290.
44. Sarhan MA. Geophysical and hydrocarbon prospect evaluation of Nukhul formation at Rabeh East oil field, Southern Gulf of Suez Basin, Egypt. *J Pet Explor Prod Technol*. 2021;11:2877–2890.
45. Sarhan MA. Geophysical assessment and hydrocarbon potential of the Cenomanian Bahariya reservoir in the Abu Gharadig Field, Western Desert, Egypt. *J Pet Explor Prod Technol*. 2021;11:3963–3993.
46. Sarhan MA, Ali AS, Abdel-Fattah MI. Geophysical assessment of basement rocks for use as an unconventional reservoir in the Rabeh East oil field, southern Gulf of Suez Basin. *Euro-Mediterranean J Environ Integration*. 2023;8:409–423.
47. Abdel-Fattah MI, Sarhan MA, Ali AS, Hamdan HA. Structural and petrophysical characteristics of the Turonian 'AR/G' reservoirs in heba field (Western Desert, Egypt): integrated approach for hydrocarbon exploration and development. *J Afr Earth Sci*. 2023;207:105072.
48. Shehata AA, Sarhan MA, Abdel-Fattah MI, Mansour S. Geophysical assessment for the oil potentiality of the Abu

Roash ‘G’ reservoir in west Beni Suef basin, western Desert, Egypt. *J Afr Earth Sci*. 2023;199:104845.
49. Hammond AL. Bright spot: better seismological indicators of gas and oil. *Science*. 1974;185:515−517.
50. Gardner GHF, Gardner LW, Gregory AR. Formation velocity and density; the diagnostic basics for stratigraphic traps. *Geophysics*. 1974;39:770−780.
51. Samuel A, Kneller B, Raslan S, Sharp A, Parsons C. Prolific deep-marine slope channels of the Nile Delta, Egypt. *AAPG Bull*. 2003;87:541−560.
52. Dolson JC, Boucher PJ, Siok J, Heppard P. Key challenges to realizing full potential in an emerging giant gas province: Nile Delta/Mediterranean offshore, deep water, Egypt. In: Doré AG, Vining BA, eds. *Petroleum Geology: North-West Europe and Global perspectives*. London: Geological Society, petroleum geology conference series no. 6, proceedings on 6th petroleum geology conference; 2005:607−624.
53. Leila M, Moscariello A. Organic geochemistry of oil and natural gas in the West Dikirnis and El-Tamad fields onshore Nile Delta, Egypt: interpretation of potential source rocks. *J Petrol Geol*. 2017;40:37−58.
54. Mohamed AAEH. *Reservoir characterization and depositional patterns of Pliocene and Miocene in the north Nile Delta, Mediterranean Sea, Egypt*. Cancun, Mexico: In American Association of Petroleum Geologist (AAPG) International Conference; 2004. October 24-27; 2004.
55. Lashin A, Mogren S. Analysis of well log and pressure data of the gas-bearing sand reservoirs of Kafr El-Sheikh formation: case study from the off-shore Nile Delta-Egypt. *Int J Phys Sci*. 2012;7:5353−5366.
56. Othman AA, Fathy M, Negm A. Identification of channel geometries applying seismic attributes and spectral decomposition techniques, Temsah Field, Offshore East Nile Delta, Egypt. *NRIAG J Astron Geophys*. 2018;7:52−61.
57. Abd El-Gawad EA, Abdelwahhab MA, Bekiet MH, Noah AZ, ElSayed NA, Abd Elhamed EF. Static reservoir modeling of El Wastani formation, for justifying development plans, using 2D seismic and well log data in Scarab field, offshore Nile Delta, Egypt. *J Afr Earth Sci*. 2019;158:103546.
58. Leila M, Mohamed A. Diagenesis and petrophysical characteristics of the shallow Pliocene sandstone reservoirs in the Shinfas Gas Field, onshore Nile Delta, Egypt. *J Pet Explor Prod Technol*. 2020;10:1−19.
59. Elatrash AM, Abdelwahhab MA, Wanas HA, El-Naggar SI, Elshayeb HM. Well log-aided source rock potential, basin modeling, and seismic attributes: petroleum geology case study of Pliocene discovery at South Mansoura Area (Nile Delta). *Arabian J Geosci*. 2021;14:1−10.
60. Abdel Aal A, El Barkooy A, Gerrits M, Meyer H, Schwander M, Zaki H. Tectonic evolution of the eastern Mediterranean Basin and its significance for the hydrocarbon prospectively in the ultra-deepwater of the Nile Delta. *Lead Edge*. 2000:1086−1102.
61. Egyptian General Petroleum (EGPC). *Nile Delta and North Sinai: Fields, Discoveries and Hydrocarbon Potential (A Comprehensive Overview)*. 1994. Cairo, Egypt.